Lithos 192–195 (2014) 132–141

Contents lists available at ScienceDirect

Lithos

journal homepage: www.elsevier.com/locate/lithos

U-series disequilibrium in young Tengchong volcanics: Recycling of mature clay sediments or mudstones into the SE Tibetan mantle

Haibo Zou [a,*], Chuan-Chou Shen [b], Qicheng Fan [c], Ke Lin [b]

[a] Department of Geology and Geography, Auburn University, Auburn, AL 36849, USA
[b] High-Precision Mass Spectrometry and Environment Change Laboratory (HISPEC), Department of Geosciences, National Taiwan University, Taipei, Taiwan, ROC
[c] Institute of Geology, China Earthquake Administration, Beijing 100029, China

ARTICLE INFO

Article history:
Received 11 August 2013
Accepted 30 January 2014
Available online 8 February 2014

Keywords:
U-series disequilibrium
Clay-rich sediments
Tengchong
Tibetan plateau
Volcanism

ABSTRACT

We report U-series disequilibrium data in the youngest volcanic rocks from Maanshan, Dayingshan and Heikongshan volcanoes in the Tengchong volcanic field, representing the only 3 volcanoes from the Indo-Asian suture zone (southwestern Tibet to western Yunnan) that are young enough to preserve ^{238}U–^{230}Th disequilibrium. The most striking feature of these young Tengchong lavas is their extremely low ($^{230}Th/^{232}Th$) (0.303 to 0.376) and ($^{238}U/^{232}Th$) (0.289 to 0.360) activity ratios (or ultra-high Th/U concentration ratio). These young lavas also show small to moderate (4% to 10%) ^{230}Th excesses. Such ^{230}Th excesses, together with tomographic results, suggest that partial melting initiated at depths greater than 75 km in the garnet stability field. U-series isotope data, together with major and trace element and Nd–Sr–Pb isotope data, indicate that Tengchong lavas are derived from partial melting of an enriched subcontinental lithospheric mantle. The ultra-high melt Th/U concentration ratios of 9.5 ± 0.7 further indicate recycling of continentally derived clay-rich mature sediments or mudstones into the SE Tibetan mantle. The materials with ultra-high Th/U ratios may come from the clay-rich mature sediments from Indian Ocean or Neo-Tethyan Ocean or the mudstones/shales from the subducted Indian continental plate.

1. Introduction

Recent extensive petrological and Nd–Sr–Pb isotopic studies of widespread Cenozoic post-collisional potassic lavas on the Tibetan Plateau (Chen et al., 2012; Chung et al., 2005; Ding et al., 2003; Flower et al., 1998; Gao et al., 2007; Guo et al., 2006; Mo et al., 2007; Turner et al., 1996; Wang et al., 2001; Williams et al., 2004; Zhou et al., 2012) have firmly established the mantle source heterogeneity below the Tibetan Plateau. However, our understanding of the melting processes and the cause of the heterogeneity in this particular tectonic setting is still unclear. In comparison to long-lived Nd–Sr–Pb isotope systems, short-lived ^{238}U–^{230}Th disequilibrium in young volcanic rocks is particularly effective and sensitive in studying melting processes due to similar short time scales between ^{238}U–^{230}Th disequilibrium and partial melting processes (Asmerom and Edwards, 1995; Elliott, 1997; McKenzie, 1985; Sims et al., 1999).

In spite of widespread presence of Cenozoic post-collisional volcanic rocks on the Tibetan Plateau, Holocene volcanism only occurred at Tengchong volcanic field in southeast Tibetan Plateau and Ashikule volcanic field in northwest Tibetan Plateau (Fig. 1). These Holocene volcanic rocks provide ideal opportunities for studying melting beneath Tibetan Plateau using ^{238}U–^{230}Th disequilibrium methods.

The Tengchong volcanic field is located along the southeastern edge of the Tibetan Plateau near the border between China and Burma (Fig. 1). The volcanism at Tengchong commenced at about 5 Ma, long after the start of the India–Asia collision (65 Ma), and has continued to the present day, spanning the entire Quaternary period (Wang et al., 2006; Zhu et al., 1983). Volcanic activity can be divided into three stages (Jiang, 1998): (1) Middle–Late Pliocene basalt, (2) Early Pleistocene pyroclastic rocks of trachydacitic composition, and (3) Holocene trachybasalts, basaltic trachyandesites, trachyandesite and trachydacites. The localities of these three Holocene (<10 ka, thousand years) volcanoes are given in Fig. 1. Several hot springs are still active in the Tengchong area and a historic (1609 AD) eruption has been reported at Dayingshan (Liu et al., 1992). A K–Ar age of groundmass from Maanshan lavas is 13 ± 6 ka (Li et al., 2000) and the thermoluminescence (TL) age of the lavas from the hilltop of the Maanshan flow is 4 ± 1 ka (Yin and Li, 2000). A similar young age was determined by ^{14}C dating (3800 ± 140 years BP) of organic matter in fluvial sediments that are overlain by a Maanshan flow. Thus, the available field observation and geochronological data are consistent with the occurrence of volcanic activity during the Holocene period. Note that for Holocene samples, the exact eruption ages are not critical as any age correction to the ^{238}U–^{230}Th disequilibrium data is minimal.

The crust below Tengchong is ~40 km thick and the structure is dominated by north–south trending strike-slip faults (Bai et al., 2001; Wang and Gang, 2004). The basement rocks are Paleozoic gneisses,

* Corresponding author. Tel.: +1 334 844 4315.
E-mail address: Haibo.zou@gmail.com (H. Zou).

0024-4937/$ – see front matter © 2014 Elsevier B.V. All rights reserved.
http://dx.doi.org/10.1016/j.lithos.2014.01.017

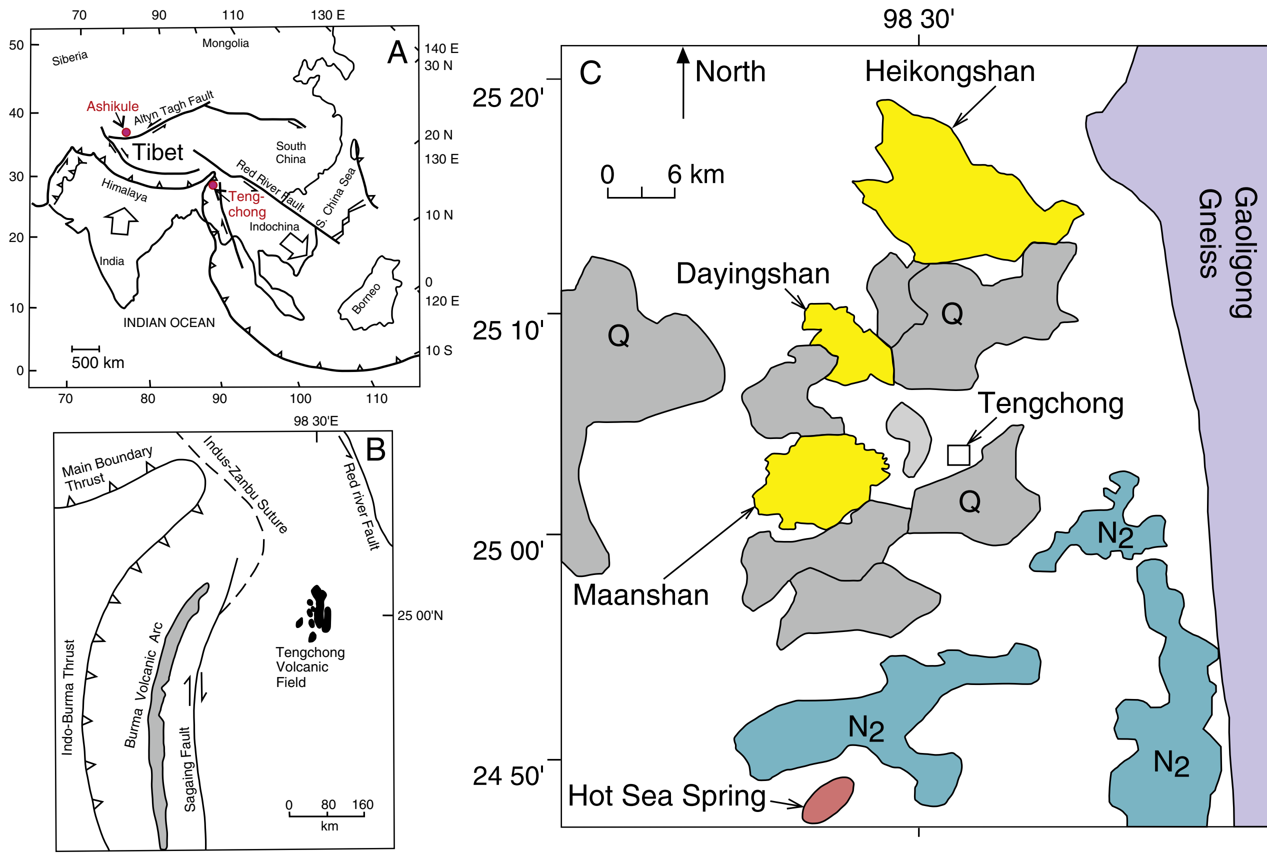

Fig. 1. (A) Regional map showing major tectonic features in Asia. Tengchong volcanic field is located on the southeast edge of the Tibetan Plateau. (B) Map showing the locality of the Tengchong volcanic field and regional tectonics. (C) Map showing the location of three young volcanoes: Maanshan, Dayingshan and Heikongshan. Q: Pleistocene volcanics; N_2: Miocene volcanics.

Carboniferous sandstones, 76 to 235 Ma Mesozoic granite and 32 to 52 Ma Cenozoic granites (Huang and Jiang, 2000).

The Holocene volcanic rocks from Tengchong are very fresh. They are fine-grained with a groundmass of volcanic glass and plagioclase microlites and porphyritic (3% to 10% clinopyroxene and plagioclase phenocrysts). Zircons have been observed in some trachyandesites (Tucker et al., 2013; Zou et al., 2010). The rocks of the Tengchong volcanic field have high-K calc-alkaline compositions. Available elemental and Nd, Sr and Pb isotopes for Tengchong volcanic rocks indicate their origin from an enriched mantle source (Chen et al., 2002; Mu et al., 1987; Wang et al., 2006; Zhou et al., 2012; Zhu et al., 1983). However, the melting processes and the characteristics of the enriched mantle are not clear. In this paper we use whole-rock ^{238}U–^{230}Th disequilibrium to provide new insights into the source characteristics, magma genesis and melting processes for the young Tengchong volcanoes. Major and trace element abundances and selected Nd, Sr and Pb isotopic compositions are also used to investigate the petrogenesis of Tengchong lavas. We will show the important role played by subducted clay-rich mature sediments, and their melts, in the formation of enriched mantle below the SE Tibetan Plateau.

2. Analytical methods

For the determination of whole-rock U–Th concentration and isotopic compositions, sample powders and spikes were digested in Teflon beakers, and U and Th were separated from matrix using a chemical procedure described in Shen et al. (2003). Isotopic measurements were conducted using a multi-collector inductively coupled plasma mass spectrometer (MC-ICP-MS), Thermo Fisher Neptune at the High-Precision Mass Spectrometry and Environment Change Laboratory (HISPEC), Department of Geosciences, National Taiwan University (Shen et al., 2012). A triple-spike, ^{229}Th–^{233}U–^{236}U, isotope dilution method was employed to correct mass bias and determine uranium concentration (Shen et al., 2002). Uncertainties in concentration and isotopic data include corrections for blanks, instrumental fractionation, multiplier dark noise, spectral interferences, and errors associated with quantifying the isotope composition in the spike solution. Table Mountain Latite (TML) is used as a rock standard. Measured ^{230}Th/^{238}U activity ratio [(^{230}Th/^{238}U)] for TML is 0.995 $\pm$ 0.005, within ^{238}U–^{230}Th secular equilibrium.

Major and trace elements were measured by XRF (Johnson et al., 1999) and quadruple ICP-MS, respectively, at the GeoAnalytical Center at the Washington State University. For trace element analysis by quadruple ICP-MS, a combination fusion–dissolution method is used in order to effectively decompose refractory mineral phases (such as zircons) and remove the bulk of unwanted matrix elements. The procedure includes a low-dilution fusion with di-lithium tetraborate for complete sample digestion, followed by an open-vial mixed acid digestion. Long-term precision for this method is typically better than 5% (RSD) for the REEs and better than 10% for other trace elements. Accuracy and precision data are listed in Table A1. Recommended values for rock standards BCR-1 and AGV-1 in Table A1 are from Govindaraju (1994).

As there are previous Nd–Sr–Pb isotope studies of Tengchong volcanic rocks, only a few samples were measured for these isotopes. Analytical methods using thermal ionization mass spectrometry have been documented elsewhere (Zou et al., 2003, 2008). Nd and Sr isotopic compositions were normalized to ^{146}Nd/^{144}Nd = 0.7219 and ^{86}Sr/^{88}Sr = 0.1194, respectively. The measured Nd and Sr isotope standard values are ^{143}Nd/^{144}Nd = 0.511843 $\pm$ 13 (n = 24) for La Jolla and ^{87}Sr/^{86}Sr = 0.710239 $\pm$ 16 (n = 13) for NBS 987. Replicate analyses of Pb isotope standard NBS 981 give ^{206}Pb/^{204}Pb = 16.896 $\pm$ 0.013, ^{207}Pb/^{204}Pb =

15.435 ± 0.014, and $^{208}Pb/^{204}Pb = 36.525 \pm 0.041$. Relative to the following values for NBS 981: $^{206}Pb/^{204}Pb = 16.9356$, $^{207}Pb/^{204}Pb = 15.4891$, and $^{208}Pb/^{204}Pb = 36.7006$ (Todt et al., 1996), Pb isotopic data in samples were corrected for mass fractionation of 0.118% per atomic mass unit (AMU) for $^{206}Pb/^{204}Pb$, 0.117% per AMU for $^{207}Pb/^{204}Pb$, and 0.119% per AMU for $^{208}Pb/^{204}Pb$. Errors of all instruments are two standard deviations (2σ) unless otherwise noted.

3. Results

3.1. Major and trace elements and Nd, Sr and Pb isotopes

Tengchong samples have SiO_2 ranging from 50.5% to 62.2% and are potassium-rich with K_2O ranging from 1.8% to 4.1% (Table 1).

In the TAS diagram (Fig. 2), after recalculation on an anhydrous basis, one sample (HE9740-1) from Heikongshan plots as a trachybasalt, two samples (MA9738-1 from Maanshan and HE1009 from Heikongshan) are basaltic trachyandesites, and all other samples classify as trachyandesites. Note that these youngest Tengchong samples span much of the compositional range of other published data for the whole Tengchong volcanic field except for the highly evolved older (1 Ma) dacites. All samples show a clear calc-alkaline trend (Fig. 3a) and belong to the high-K calc-alkaline series (Fig. 3b). They are not shoshonites, unlike much of the volcanism on the main parts of the Tibetan Plateau.

The Tengchong samples are enriched in incompatible elements. All samples show LREE enrichment over HREE (Fig. 4). Except for two samples with low SiO_2 from Heikongshan, all samples display moderate negative Eu anomalies, indicating fractional crystallization of plagioclase. In the normalized trace element diagram (Fig. 5), all samples have pronounced positive peaks in Th and negative anomalies in Nb and Ta.

Nd, Sr and Pb isotope data for our samples are within the range previously reported for Tengchong Holocene and pre-Holocene lavas (Chen et al., 2002; Wang et al., 2006; Zhao and Fan, 2010; Zhu et al., 1983). The Tengchong samples have high $^{87}Sr/^{86}Sr$ and low $^{143}Nd/^{144}Nd$ (Fig. 6). Their ε_{Nd} varies from −4.4 to −10.1, showing enriched characteristics.

The Tengchong volcanics have highly radiogenic $^{208}Pb/^{204}Pb$ (39.1 to 39.3) and $^{207}Pb/^{204}Pb$ (15.65 to 15.70) but relatively unradiogenic $^{206}Pb/^{204}Pb$ (18.1 to 18.2). Pb radiogenic ratio $^{208}Pb^{*}/^{206}Pb^{*}$ (Allegre et al., 1986) is considered as an indicator of Th/U ratios on the time scale of hundreds of millions of years. The Tengchong samples have $^{208}Pb^{*}/^{206}Pb^{*}$ of 1.09 to 1.10, indicating long-term Th enrichment over U. Time-integrated $^{232}Th/^{238}U$ in the source, κ_{Pb} from Pb isotopes (Galer and O'Nions, 1985), is 4.4 to 4.5, significantly lower than κ_{Th} from Th isotopes (ranging from 8.3 to 10.3). κ_{Th} from Th isotopes represents recent $^{232}Th/^{238}U$ while κ_{Pb} from Pb isotopes represents long-term $^{232}Th/^{238}U$.

3.2. ^{238}U–^{230}Th disequilibrium

U–Th isotope data are presented in Table 2. The most striking feature of the U–Th data is their extremely low ($^{230}Th/^{232}Th$) and ($^{238}U/^{232}Th$) ratios (Fig. 7), as compared to the values of the continental volcanic rocks from NE China (including Wudalianchi, Jingbohu, Longgang, and Changbaishan) (Zou et al., 2003, 2008), Hainan Island (Zou and Fan, 2010) and Ashikule volcanics from northern Tibet (Cooper et al., 2002). The Tengchong volcanic rocks have ($^{230}Th/^{232}Th$) ratios ranging from 0.303 to 0.376 and ($^{238}U/^{232}Th$) ratios ranging from 0.289 to 0.360.

Peate and Hawkesworth (2005) summarized the ($^{238}U/^{232}Th$) values for lavas formed in various tectonic setting. MORB lavas have ($^{238}U/^{232}Th$) between 0.9 and 1.6, subduction zone lavas have a wide range of ($^{238}U/^{232}Th$) from 0.4 to 3.4, and within-plate lavas have ($^{238}U/^{232}Th$) ranging from 0.4 to 1.2 (Peate and Hawkesworth, 2005). Among within-plate lavas, continental potassic lavas have the lowest ($^{238}U/^{232}Th$) between 0.4 and 0.7. For example, the ($^{238}U/^{232}Th$) values are 0.396 to 0.421 for Gaussberg from Antarctica, 0.497 to 0.553 for Ashikule lavas from N Tibet (Cooper et al., 2002), 0.605 to 0.683 for Wudalianchi lavas (Zou et al., 2003), and 0.648 for Nyamuragira lavas from East Africa (Pickett and Murrell, 1997). Note that the ($^{238}U/^{232}Th$) values between 0.289 and 0.360 for Tengchong lavas from SE Tibet are lower than reported values for young lavas from various tectonic settings (intraplate, convergent margins and divergent margins) (Bourdon and Sims, 2003; Lundstrom, 2003; Turner et al., 2003), including the Toba lavas from Sunda arc known for low ($^{238}U/^{232}Th$) values (as low as 0.438) (Turner and Foden, 2001).

Since κ_{Th} is defined as ($^{232}Th/^{230}Th$)$\lambda_{238}/\lambda_{232}$ (Galer and O'Nions, 1985), the Tengchong lavas have very high κ_{Th}, ranging from 8.3 to 10.3 (Galer and O'Nions, 1985). Note that k represents $^{232}Th/^{238}U$ ratio, and κ_{Th} from Th isotopes represents recent $^{232}Th/^{238}U$ in equilibrium with ($^{230}Th/^{232}Th$).

4. Discussion

4.1. Crustal contamination or mantle metasomatism?

One of the most challenging problems in the study of lavas from continental setting is how to rigorously evaluate the potential role and extent of crustal contamination during magma ascent. This assessment is especially needed for the potassic lavas from Tengchong with low ε_{Nd} (−7) and high $^{87}Sr/^{86}Sr$ (0.707).

The predominant country rocks in Tengchong are granites, granodiorites, and amphibolites and these all have $^{206}Pb/^{204}Pb$ ratios higher than those of the Tengchong volcanic rocks (Chen et al., 2002). The Southeast Asian mantle source represented by the Thailand basalts also has $^{206}Pb/^{204}Pb$ ratios higher than those of the Tengchong volcanic rocks (Mukasa et al., 1996). Therefore, mixing of the Southeast Asian mantle source with any of the above country rocks cannot explain the Nd–Pb isotope systematics of the Tengchong volcanics (Fig. 8). As previously proposed by Chen et al. (2002), the Pb–Sr isotopic systematics of the Tengchong lavas (Fig. 4 in Chen et al., 2002) also do not support significant crustal contamination during magma ascent.

^{238}U–^{230}Th ages of zircons from Tengchong lavas provide significant insights into potential crustal contamination. Zircons from Maanshan volcano have two age populations at 91 ka and 55 ka, significantly younger than any country rocks (ranging from Paleozoic to 32 Ma) (Zou et al., 2010). Zircons from Dayingshan volcano also have ages of 58 ka and 88 ka (Tucker et al., 2013). The absence of xenocrystic zircons older than 300,000 years strongly suggests that crustal contamination during the ascent of Tengchong magmas is not significant. Note that the lithology of the country rocks, including Paleozoic gneisses, Carboniferous sandstones, 76 to 235 Ma Mesozoic granite and 32 to 52 Ma Cenozoic granites, is zircon rich. Thus, both Pb isotope compositions and young ages of zircons from the Tengchong lavas do not support significant crustal contamination. The enriched characteristics of the Tengchong volcanic rocks are most likely inherited from partial melting of an enriched mantle source.

4.2. ^{238}U–^{230}Th disequilibrium and mantle melting

The Maanshan volcano and Dayingshan volcano display small ^{230}Th excesses (4% to 6%) and the Heikongshan volcano has moderate ^{230}Th excesses (6% to 11%), which is in contrast with significant ^{230}Th excesses in many primitive Holocene volcanic rocks from NE China (mostly 20% to 33% ^{230}Th excesses) and Hainan Island (18% to 32% ^{230}Th excesses). The ages of young zircon phenocrysts at Maanshan and Dayingshan are 55 ka (Tucker et al., 2013; Zou et al., 2010) and can be regarded as the age of magma formation (magma residence time + eruption age). If we correct Tengchong Holocene lavas with magma formation time of 55 ka (instead of eruption ages of <10 ka in Holocene), then all samples had original 6%–10% ^{230}Th excesses, except for one sample (HS-9740-8) from Heikongshan with original 18% ^{230}Th excess. The

Table 1
Major and trace element concentrations and Nd, Sr, Pb isotopic compositions.

Sample	Maanshan					Daying		
	MN-9704-1	MN-9704-1R	MS-9738-1	MSW-9738-10	Ma2010-1	DSE-9723-2	DNW-9724-1	DNW-9724-2
SiO2	57.60		51.90	58.36	57.85	58.11	59.07	61.67
TiO2	1.20		1.45	1.13	1.23	1.10	1.13	0.98
Al2O3	16.63		17.04	16.36	16.91	16.81	16.49	16.05
FeO	6.03		9.32	6.23	6.08	6.34	6.88	5.70
MnO	0.11		0.16	0.09	0.11	0.10	0.10	0.09
MgO	3.62		5.49	3.18	3.49	2.68	2.91	2.35
CaO	5.62		7.99	3.18	6.04	4.84	5.23	4.30
Na2O	3.81		3.42	3.43	3.79	3.08	3.42	3.29
K2O	3.35		1.79	3.57	3.34	3.58	3.59	4.05
P2O5	0.47		0.34	0.43	0.48	0.43	0.45	0.38
Loss			0.80	1.03	0.40	2.31	0.47	0.69
Total	98.43		99.70	99.37	99.73	99.38	100.03	99.55
$K_2O + Na_2O$	7.16		5.21	7.00	7.13	6.66	7.01	7.34
FeO*/MgO	1.67		1.70	1.96	1.74	2.36	2.36	2.43
La	63.65	63.89	67.50	66.12	66.15	81.37	78.70	81.51
Ce	121.19	121.73	126.20	123.84	124.03	154.08	148.46	155.38
Pr	13.15	13.17	13.85	13.49	13.61	16.92	16.32	16.63
Nd	47.22	47.23	48.64	47.92	48.57	59.29	57.64	58.28
Sm	8.52	8.49	8.59	8.40	8.52	10.17	9.97	9.81
Eu	1.95	1.92	1.90	1.84	2.01	2.07	2.11	1.90
Gd	6.96	6.82	6.75	6.76	6.71	7.68	7.57	7.59
Tb	1.02	1.01	1.00	0.99	1.01	1.11	1.08	1.11
Dy	5.87	5.77	5.75	5.62	5.80	6.19	6.14	6.07
Ho	1.11	1.11	1.09	1.08	1.13	1.15	1.15	1.16
Er	2.96	2.89	2.90	2.88	2.98	2.98	2.96	2.97
Tm	0.42	0.41	0.43	0.41	0.43	0.43	0.42	0.42
Yb	2.55	2.57	2.53	2.54	2.62	2.57	2.52	2.65
Lu	0.39	0.40	0.39	0.41	0.41	0.40	0.39	0.40
Ba	794	797	780	929	801	1020	1013	882
Th	22.55	22.71	23.85	24.83	21.44	29.66	26.03	32.47
Nb	27.69	27.69	26.71	27.07	27.63	28.43	27.99	27.54
Y	28.34	28.07	28.32	28.19	29.38	29.87	29.58	29.74
Hf	6.38	6.42	6.45	6.52	6.48	8.10	8.07	8.01
Ta	2.12	2.15	1.64	2.40	1.63	1.80	1.66	1.69
U	2.53	2.55	2.61	2.71	2.43	2.82	2.57	3.12
Pb	17.20	17.48	20.26	20.70	18.47	25.95	23.94	24.91
Rb	97.4	99.0	102.8	105.5	94.8	116.5	107.7	140.1
Cs	1.05	1.08	1.75	1.77	1.33	2.35	1.36	1.83
Sr	590	587	560	540	601	510	549	475
Sc	14.1	14.7	14.0	14.5	15.3	12.7	13.6	11.3
Zr	254	255	252	254	272	314	312	308
Th/U	8.9	8.9	9.1	9.2	8.8	10.5	10.1	10.4
Ce/Pb	7.0	7.0	6.2	6.0	6.7	5.9	6.2	6.2
Nb/U	10.9	10.9	10.2	10.0	11.4	10.1	10.9	8.8
Ba/Th	35	35	33	37	37.4	34	39	27
Sr/Th	26	26	23	22	28	17	21	15
Sr/Y	21	21	20	19	20	17	19	16
$^{87}Sr/^{86}Sr$	0.707540		0.706583	0.707545			0.708782	
2SE	0.000012		0.000013	0.000009			0.000009	
$^{143}Nd/^{144}Nd$	0.512282		0.512370	0.512263			0.512187	
2SE	0.000007		0.000014	0.000008			0.000013	
Epsilon Nd	−6.9		−5.2	−7.3			−8.8	
$^{206}Pb/^{204}Pb$	18.161			18.133			18.186	
$^{207}Pb/^{204}Pb$	15.684			15.653			15.709	
$^{208}Pb/^{204}Pb$	39.190			39.090			39.256	
$^{208}Pb^*/^{206}Pb^*$	1.10			1.09			1.10	
K_{Pb}	4.47			4.43			4.47	

minor to moderate ^{230}Th excesses from all three youngest volcanoes at Tengchong may suggest the dominant role of mantle decompression melting rather than fluid addition in magma generation. The association of such ^{230}Th excesses with lavas erupted through thick continental crust rather than thin oceanic crust is consistent with the influence of the thickness of the overlying lithosphere on the mantle dynamics and partial melting within the wedge (George et al., 2003; Peate and Hawkesworth, 2005; Plank and Langmuir, 1988; Turner et al., 2003). Although direct slab melting may explain the ^{230}Th excesses of lavas in the Austral Andes (Sigmarsson et al., 1998) and in the central Kamchakan (Dosseto et al., 2003) where the subducting slab is young and hot, the slab beneath Tengchong is an old one. Thus we attribute the ^{230}Th excesses in Tengchong lavas to mantle decompression melting rather than direct slab melting.

The mantle minerals that control U and Th partitioning during partial melting are clinopyroxene and garnet. Garnet is the dominant mineral phase in the mantle where thorium is significantly more incompatible than uranium ($D_{Th} < D_U$) during mantle melting (Beattie, 1993; LaTourrette et al., 1993; Salters and Longhi, 1999). Partial melting of garnet peridotites in the garnet stability field (>2.5 GPa, or 75 km) can produce ^{230}Th excesses. As for clinopyroxene, high-Al_2O_3 clinopyroxene can produce ^{230}Th excesses at pressure >1.5 GPa (about 50 km depth),

Daying		Heikong				
DC-9724-5	DA-09026	HS-9719-1	HS-9719-1R	HE-9740-1	HS-9740-8	HE-10009
62.24	61.50	60.91	60.71	50.47	58.43	54.36
0.93	1.01	0.98	0.97	1.41	1.10	1.43
16.01	16.27	15.28	15.24	17.75	16.36	17.26
5.45	5.22	5.03	5.03	8.62	6.12	8.17
0.09	0.092	0.09	0.09	0.14	0.11	0.14
2.14	2.43	2.81	2.81	5.76	3.73	4.5
4.11	4.54	4.39	4.36	6.69	5.56	6.84
3.42	3.60	3.47	3.45	3.08	3.48	4.03
4.09	4.02	3.90	3.87	2.19	3.43	2.7
0.35	0.40	0.68	0.68	0.36	0.42	0.39
0.43				3.38	0.56	
99.26	99.09	97.55	97.21	99.85	99.30	99.82
7.51	7.62	7.37	7.32	5.27	6.91	6.73
2.55	2.14	1.79	1.79	1.50	1.64	1.82
79.22	86.76	67.66		34.62	72.64	46.13
151.39	166.35	128.41		66.48	137.43	88.38
16.37	17.77	14.04		7.52	14.92	9.97
57.19	61.53	49.15		28.25	54.07	36.10
9.79	10.38	8.75		5.83	9.34	6.92
1.82	1.98	1.70		1.64	2.01	1.81
7.40	7.57	6.78		5.53	7.20	6.20
1.08	1.12	0.99		0.88	1.03	0.99
5.97	6.16	5.53		5.23	5.74	5.88
1.14	1.17	1.06		1.06	1.09	1.17
3.00	3.06	2.70		2.74	2.81	3.09
0.43	0.44	0.39		0.39	0.39	0.44
2.60	2.63	2.44		2.42	2.37	2.69
0.40	0.41	0.38		0.37	0.36	0.42
865	933	836		453	930	521.00
34.32	33.48	28.58		12.14	21.85	17.78
27.60	28.47	27.51		21.07	27.97	23.41
29.27	30.14	27.06		26.33	27.56	29.94
8.13	8.06	7.79		4.47	7.81	5.28
2.69	1.76	1.71		1.27	2.47	1.40
3.32	3.22	3.28		1.33	2.41	1.73
25.57	26.67	26.51		9.26	19.90	13.15
150.3	136.5	136.0		43.8	101.9	57.20
2.02	1.72	1.79		1.21	1.05	0.70
445	457	419		475	556	451
10.9	13.5	12.9		21.2	14.5	20.7
303	329	300		181	308	225
10.3	10.4	8.7		9.1	9.1	10.3
5.9	6.2	4.8		7.2	6.9	6.7
8.3	8.9	8.4		15.9	11.6	13.5
25	28	29		37	43	29
13	14	15		39	25	25
15	15	16		18	20	15
0.708971				0.705723	0.708553	
0.000013				0.000013	0.000011	
0.512121				0.512410	0.512213	
0.000014				0.000014	0.000012	
−10.1				−4.4	−8.3	
					18.044	
					15.647	
					39.051	
					1.10	
					4.45	

but generate ^{238}U excesses at pressure <1.5 GPa (Landwehr et al., 2001; Wood et al., 1999). Unlike high Al_2O_3 clinopyroxene, calcic clinopyroxene consistently produces ^{238}U excesses. The ^{230}Th excesses in the Tengchong lavas suggest melting in the presence of high-pressure aluminous clinopyroxene (at depth greater than 50 km depth) and/or in the presence of garnet at depth greater than 75 km to 90 km. Note that these Tengchong volcanics also have relatively high Sr/Y ratios ranging from 15 to 21 (Table 1), consistent with deep melting with garnet as a residual phase, as garnet retains Y but Sr goes into melt.

We suggest that partial melting initiated in the presence of garnet at depths greater than 75 km to 90 km. This is supported by recent tomographical studies that have revealed a low-velocity zone at depths up to 150 km (Li et al., 2008) to 300 km (Huang and Zhao, 2006; Lei et al., 2013) below Tengchong. If the low-velocity zone represents melt generation zone for Tengchong volcanoes, then the ^{230}Th excesses in the Tengchong lavas mostly likely indicate partial melting in the upper mantle in the garnet stability field. Note that trace element inversion results also support for a role of residual garnet in the source region during melting in some areas of the main Tibetan Plateau (Gao et al., 2009; Williams et al., 2004).

In comparison with the Tengchong volcanics from SE Tibetan Plateau, the Ashikule volcanics from NW Tibetan Plateau (Fig. 1) display

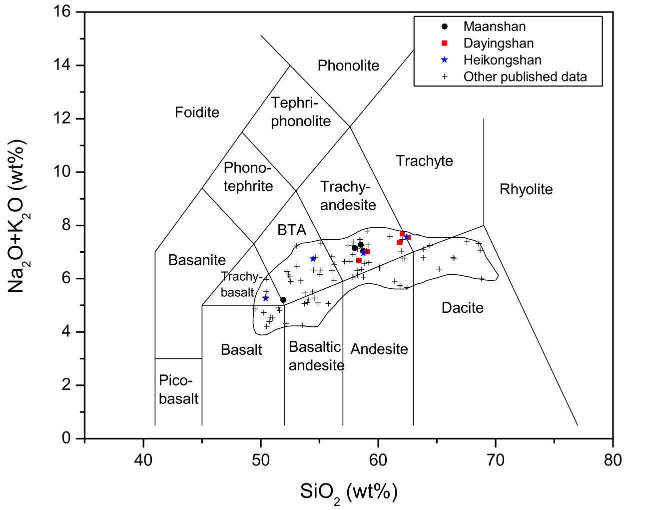

Fig. 2. Total alkali (K_2O + Na_2O) versus SiO_2 for the volcanic rocks from Maanshan, Dayingshan and Heikongshan of Tengchong. Data sources for other published Tengchong volcanic rocks: Wang et al. (2006), Zhao and Fan (2010), Zhou et al. (2012), Zhu et al. (1983), Zou et al. (2010). Major element data have been recalculated on a volatile free basis.

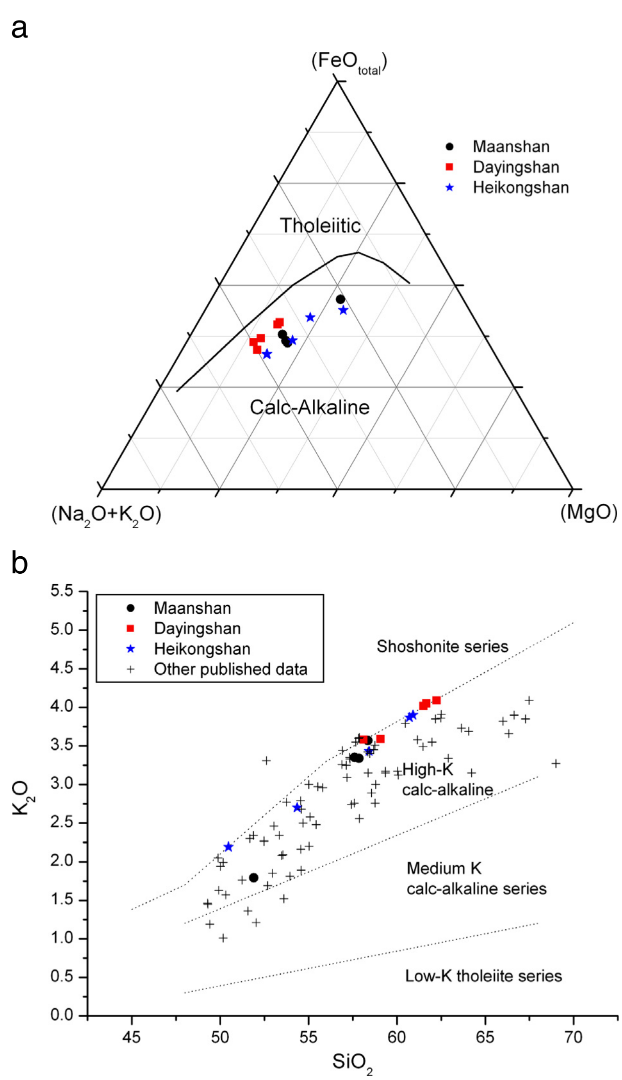

Fig. 3. (a) AFM diagram for Maanshan, Dayingshan, and Heikongshan. (b) K_2O versus SiO_2 diagram.

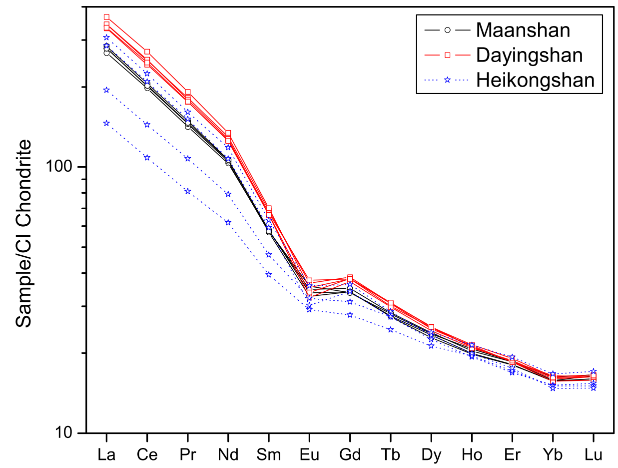

Fig. 4. Chondrite-normalized rare earth element diagram for Maanshan, Dayingshan, and Heikongshan.

more pronounced initial ^{230}Th (mostly 14% to 36%) excesses (Cooper et al., 2002). It is therefore likely that the melting conditions to generate Tengchong and Ashikule volcanics were different. The Tengchong lavas with smaller ^{230}Th excesses were generated by faster melting rates and higher melting porosities as compared with the Ashikule lavas (Fig. 9).

4.3. Ultra-high Th/U magmas and metasomatism by subducted clay-rich sediments

All Tengchong samples have very high Th/U ratios. Their Th/U ratios measured at National Taiwan University by isotope dilution MC-ICP-MS and at Washington State University by quadrupole ICP-MS using separate sample dissolutions are identical within 5%. Before we attribute their high Th/U ratios to their mantle source characteristics, we need to demonstrate that their high Th/U ratios do not result from (1) incomplete zircon dissolution and (2) crustal-level fractionation of zircons. Because zircons have low Th/U ratios, incomplete zircon dissolution or crustal-level fractionation of zircons increases Th/U ratios in melts. However, there is no correlation between Th/U and SiO_2 (Fig. 10) for the Tengchong lavas. Th/U ratios in zircon-containing samples with high SiO_2 are similar to those zircon-absent samples with low SiO_2, which argues against incomplete zircon dissolution or crustal-level fractionation of zircons.

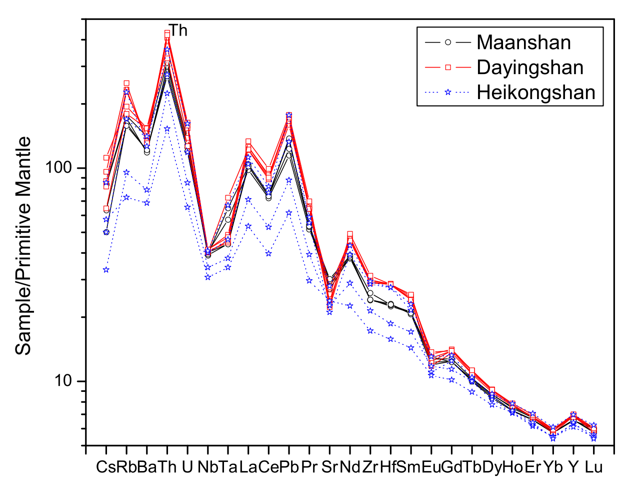

Fig. 5. Primitive mantle normalized trace element diagram for Maanshan, Dayingshan and Heikongshan.
Normalizing values are from McDonough and Sun (1995).

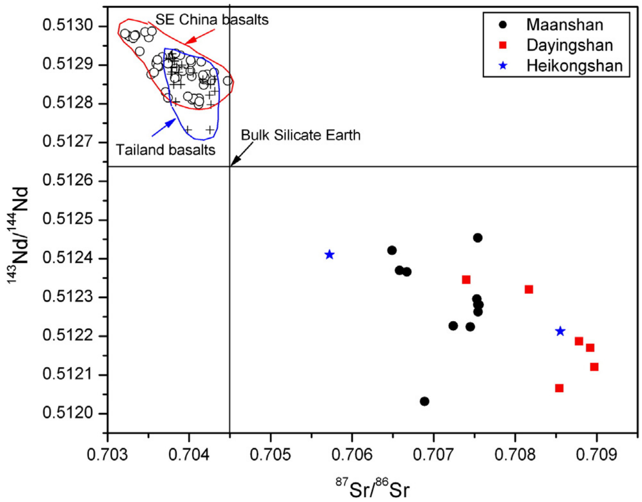

Fig. 6. $^{143}Nd/^{144}Nd$ versus $^{87}Sr/^{86}Sr$ diagram. DMM = depleted MORB mantle (Zindler and Hart, 1986); SE China basalts (Tu et al., 1991; Zou and Fan, 2010; Zou et al., 2000); Thailand basalts (Mukasa et al., 1996).

Dynamic partial melting (McKenzie, 1985) or porous flow (Spiegelman and Elliott, 1993) may significantly fractionate ^{230}Th from ^{238}U owing to the ^{230}Th ingrowth from parental ^{238}U. However, these processes do not significantly fractionate ^{232}Th from ^{238}U (Williams et al., 1992; Zou and Zindler, 2000). Unlike ^{230}Th, ^{232}Th has no parent–daughter relationship with ^{238}U and thus no ingrowth during melting and transport. Therefore, the ultra-high elemental Th/U ratios in Tengchong lavas cannot be caused by Th/U partitioning during partial melting or melt transport, but are likely to reflect the characteristics of the mantle source itself.

The Tengchong lavas have ultra-high Th/U ratios (9.50 ± 0.69), even higher than some well-known high Th/U lavas, such as Gaussberg lavas (7.55 ± 0.05) (Williams et al., 1992), Ashikule lavas (5.80 ± 0.20) (Cooper et al., 2002) and Wudalianchi lavas (4.65 ± 0.18) (Zou et al., 2003). In comparison, continental upper crust, middle crust and lower crust have average Th/U ratios of 3.8, 4.9 and 6.0, respectively (Rudnick and Gao, 2003) and bulk silicate earth has Th/U ratio of 3.9 (McDonough and Sun, 1995).

Since subduction-related fluids are enriched in U relative to Th, the ultra-high Th/U ratios in the Tengchong lavas do not suggest significant fluid additions. Instead, the ultra-high Th/U ratios may indicate contributions from sediment melts with high Th/U ratios.

Our data can provide further insights on the lithology of the subducted sediments. Th/U ratios in subducting sediments can vary from greater than 10 to less than 1 (Plank and Langmuir, 1998). High Th/U ratios reflect a mature weathered source whereas low Th/U ratios indicate immature continental sediments or organic rich sediments (Plank and Langmuir, 1998). Such ultra-high Th/U sediments must be clay-rich mature sediments or mudstones, because clay-rich mature sediments or mudstones might be the main mature sediments with very high Th/U ratios after extensive weathering to remove U and retain Th. For example, pelagic clays from Indian Ocean have Th/U ratios of 9.0–10.5 (Ben Othman et al., 1989). A recent high-pressure experimental study (Rapp et al., 2008) indicates the formation of high Th/U K-hollandite from a marine mud sample in the deep mantle. Neither sandstones nor limestones have high Th/U ratios. Thus, our study provides strong evidence for recycling of clay-rich mature sediment or mudstone melts into the mantle source to form enriched mantle below Tengchong.

Melts derived from such subducted clay-rich sediments may react with depleted mantle at depth, producing phlogopite-bearing pyroxenites at the expense of olivine (Prelevic et al., 2013; Sekine and Wyllie, 1983). This process results in regions of heterogeneous mantle consisting of enriched phlogopite- and garnet-bearing pyroxenites within depleted peridotite mantle in the subcontinental lithospheric mantle. Deep melting of such heterogeneous mantle produces moderate ^{230}Th excesses.

The mantle beneath the Tibetan Plateau was affected by Neo-Tethyan oceanic subduction prior to the collision of India and Asia and was followed by the subduction of Indian continental crust beneath Asia after the collision (Mo et al., 2007; Zhao et al., 2009). The Tengchong region of SE Tibetan Plateau is different because, unlike other parts of the Tibetan Plateau, subduction of the Indian continental crust was followed by the subduction of the Indian oceanic plate beneath Tengchong and Burma. A stagnant slab with high-V anomaly in the mantle transition zone below Tengchong as detected by seismic imaging (Lei et al., 2009, 2013; Zhao and Liu, 2010) might represent the subducted Indian oceanic slab. The clay-rich sediment melt component in the Tengchong lavas may be derived from the stagnant slab beneath Tengchong and/or from the earlier subduction of Indian continental crust. The inferred Precambrian Nd model age (1.1 Ga) may actually reflect the inheritance of isotopic signatures from melts derived from such subducted clay-rich sediments, rather than the time when the

Table 2
Uranium and thorium isotopic compositions.

Sample ID	U, ppm	Th, ppm	($^{238}U/^{232}Th$)	($^{230}Th/^{232}Th$)	($^{234}U/^{238}U$)	($^{230}Th/^{238}U$)	K_{Th}
Maanshan							
MN-9704-1	2.30 ± 0.01	19.67 ± 0.03	0.355 ± 0.002	0.373 ± 0.002	1.016 ± 0.012	1.048 ± 0.007	8.39
MSW-9738-1	2.291 ± 0.007	19.96 ± 0.03	0.348 ± 0.001	0.364 ± 0.002	0.975 ± 0.009	1.046 ± 0.006	8.58
MSW-9738-1[a]	2.34 ± 0.02	20.6 ± 0.2	0.346 ± 0.005	0.359 ± 0.004	–	1.04 ± 0.02	8.73
MA2010-1	2.104 ± 0.006	17.71 ± 0.03	0.360 ± 0.001	0.374 ± 0.002	1.003 ± 0.005	1.037 ± 0.006	8.37
Dayingshan							
DSE9723-2	2.689 ± 0.008	26.81 ± 0.03	0.304 ± 0.001	0.323 ± 0.002	0.989 ± 0.007	1.061 ± 0.006	9.67
DNW-9724-1	2.520 ± 0.005	23.76 ± 0.08	0.322 ± 0.001	0.338 ± 0.002	0.998 ± 0.006	1.050 ± 0.007	9.25
DNW-9724-2	3.040 ± 0.007	30.89 ± 0.04	0.299 ± 0.001	0.310 ± 0.002	0.978 ± 0.006	1.038 ± 0.006	10.1
DC-9724-5	2.939 ± 0.007	30.88 ± 0.04	0.289 ± 0.001	0.303 ± 0.002	–	1.048 ± 0.006	10.3
Heikongshan							
HE-9740-1	1.312 ± 0.006	11.88 ± 0.01	0.335 ± 0.002	0.356 ± 0.002	1.020 ± 0.008	1.062 ± 0.008	8.78
HS-9740-8	2.602 ± 0.009	23.21 ± 0.03	0.340 ± 0.001	0.376 ± 0.002	1.000 ± 0.011	1.107 ± 0.007	8.30
TML	9.64 ± 0.02	27.29 ± 0.03	1.072 ± 0.002	1.067 ± 0.005	1.002 ± 0.005	0.995 ± 0.005	2.93

Chemistry was performed following methods in Shen et al. (2003), and instrumental analysis on MC-ICP-MS (Shen et al., 2012).
Analytical errors are 2σ of the mean.
Activity ratios calculated using decay constants of 9.1577×10^{-6} year^{-1} for ^{230}Th, 4.9475×10^{-11} year^{-1} for ^{232}Th, 2.8263×10^{-6} year^{-1} for ^{234}U (Cheng et al., 2000), and 1.55125×10^{-10} year^{-1} for ^{238}U (Jaffey et al., 1971).
TML: Table Mountain Latite, a rock reference material for uranium-series community.
[a] A duplicate measured at UCLA using TIMS (from separate dissolution).

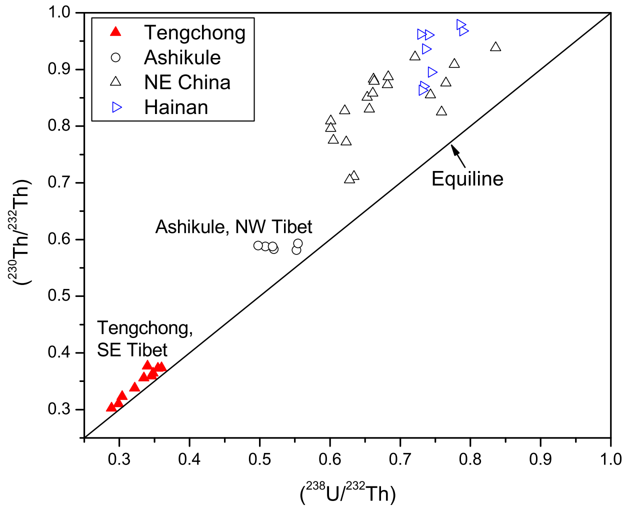

Fig. 7. (^{230}Th/^{232}Th) versus (^{238}U/^{232}Th) equiline diagram. Data sources: this paper; Cooper et al. (2002), Zou and Fan (2010), Zou et al. (2008), Zou et al. (2003). Decay constants: Cheng et al. (2000), Jaffey et al. (1971).

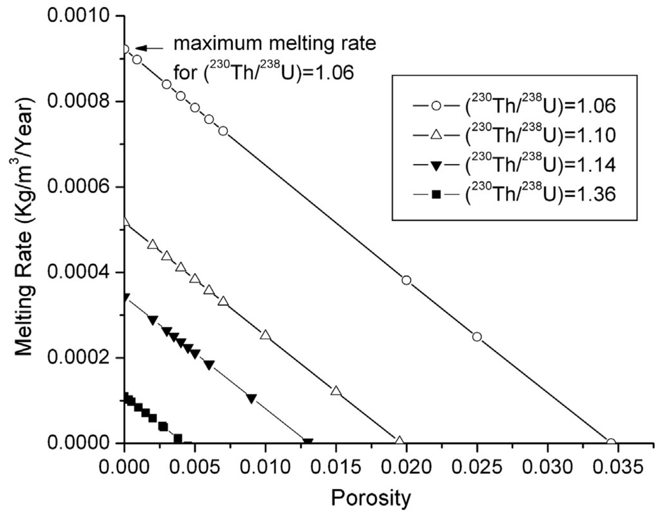

Fig. 9. Estimates of maximum melting rate and maximum melting porosity from U–Th disequilibrium data (Zou, 2007) for Tengchong and Ashikule volcanics. Most Tengchong volcanics have initial (^{230}Th/^{238}U) of 1.06 to 1.10 and most Ashikule volcanics have initial (^{230}Th/^{238}U) of 1.14 to 1.36. Bulk partition coefficients are $D_U = 0.005$ and $D_{Th} = 0.003$ for garnet peridotites. Bulk partition coefficients are given by $D_i = \sum K_i x_i$, where K_i is the mineral/melt partition coefficient, and x_i is its mineral proportion in the source. Mineral/melt partition coefficients are: $K_{Th}(gt) = 0.019$, $K_U(gt) = 0.041$, $K_{Th}(opx) = 0.0002$, $K_U(opx) = 0.0005$ (Salters and Longhi, 1999), $K_{Th}(cpx) = 0.015$, $K_U(cpx) = 0.010$ (Lundstrom et al., 1994), and $K_{Th}(ol) = K_U(ol) = 0.0001$ (assumed). Mineral proportions are: $x_{ol} = 61\%$, $x_{opx} = 22\%$, $x_{gt} = 10\%$, and $x_{cpx} = 7\%$. Mineral abbreviations: gt = garnet, opx = orthopyroxene, cpx = clinopyroxene, and ol = olivine. Melting of a garnet pyroxenite source (with more garnet) rather than a garnet peridotite source would imply higher melting rate and/or porosity for a given (^{230}Th/^{238}U).

lithosphere became isolated from asthenospheric convection. Because of the extremely complex Phanerozoic tectonic and magmatic evolution of Tibet (Ding et al., 2003), it is unlikely that enriched Precambrian mantle lithosphere has remained geochemically isolated and physically intact beneath Tibet for more than 1 Gyr. The composition of any pre-existing Precambrian mantle lithosphere would have been altered by the northward subduction of the Tethyan oceanic lithosphere beneath Tibet during the Mesozoic. In addition, the complete lack of correlation between Th/U and ^{208}Pb*/^{206}Pb* also argues for a young mantle source. We note that some older volcanic rocks on Tibetan Plateau also have very high Th/U ratios. Although they are too old to preserve ^{238}U–^{230}Th disequilibrium, their high Th/U ratios may also indicate that their mantle sources may be also related to the subduction of mature clay-rich sediments or mudstones.

5. Conclusions

1. The Tengchong samples are characterized by their extremely low (^{230}Th/^{232}Th) and (^{238}U/^{232}Th) ratios. They display small to moderate (4% to 10%) ^{230}Th excesses.
2. The ^{230}Th excesses in the Tengchong lavas, along with geophysical data, suggest that melting initiated at depths greater than 75 km in the garnet stability field.
3. The ultra-high Th/U ratios in Tengchong lavas indicate recycling of continentally-derived clay-rich mature sediments into the mantle. The Tengchong lavas are derived from the lithospheric mantle that had been metasomatized by clay-rich sediment melts prior to melting. The high ^{208}Pb/^{204}Pb, high ^{87}Sr/^{86}Sr and low ^{143}Nd/^{144}Nd

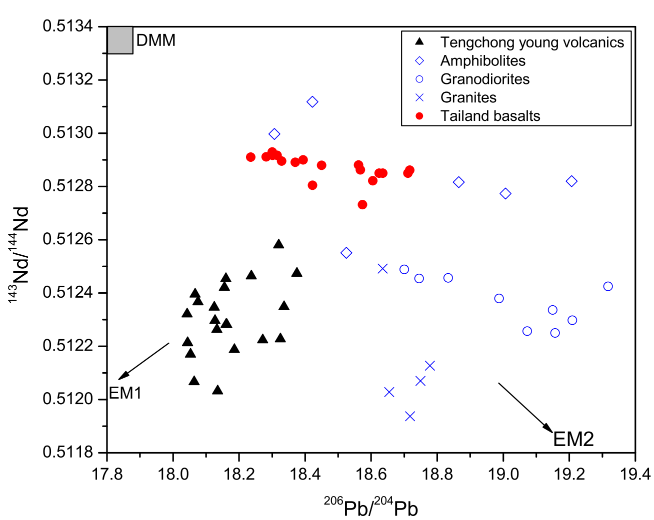

Fig. 8. ^{143}Nd/^{144}Nd versus ^{206}Pb/^{204}Pb diagram. Data sources: Tengchong volcanic rocks (this paper; Chen et al., 2002; Wang et al., 2006; Zhao and Fan, 2010; Zou et al., 2003); local crustal materials of amphibolites, granodiorites and granites (Chen et al., 2002); Thailand basalts (Mukasa et al., 1996). Since Nd and Pb concentrations for local crustal materials are not available in Chen et al. (2002), quantitative mixing curves are not calculated here.

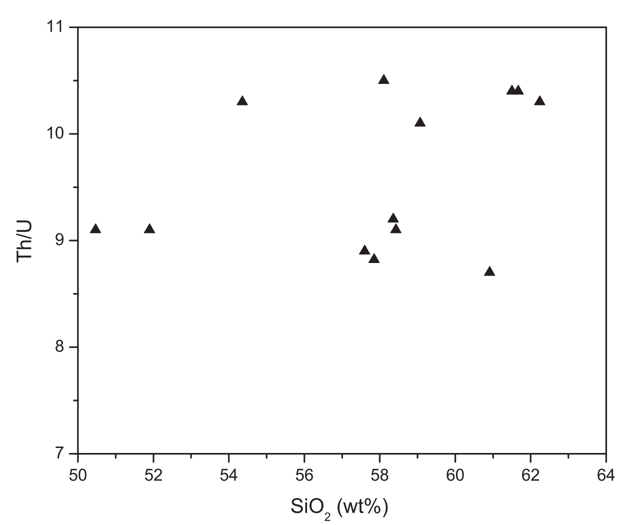

Fig. 10. Th/U versus SiO_2 plot.

ratios of the Tengchong lavas may reflect inheritance from clay-rich sediments that were derived from pre-existing continental crust.

Supplementary data to this article can be found online at http://dx.doi.org/10.1016/j.lithos.2014.01.017.

Acknowledgments

David Peate, Simon Turner and journal editor Andrew Kerr provided very constructive reviews that have significantly improved the quality of this paper. Zou thanks Zhong-zhe Zhou for his assistance and hospitality during Zou's visit at NTU. We are also grateful to Dr. Zhengfu Guo for providing several samples, Charles Knaack for providing excellent ICP-MS analyses, and Mingjia Ma for drawing Fig. 1. This study was supported by the US NSF (EAR 1119077 and EAR 0917561), National Natural Science Foundation of China (41272070), and Auburn University IGP Grant 2011-3-18. MC-ICP-MS measurement of U–Th isotopic compositions at the HISPEC was supported by the ROC NSC and NTU grants (100-2116-M-002-009, 101-2116-M-002-009 and 101R7625 to CCS).

References

Allegre, C.J., Dupre, B., Lewin, E., 1986. Thorium/uranium ratio of the Earth. Chemical Geology 56, 219–227.

Asmerom, Y., Edwards, R.L., 1995. U-series isotope evidence for the origin of continental basalts. Earth and Planetary Science Letters 134, 1–7.

Bai, D., Meju, M.A., Liao, Z., 2001. Magnetotelluric images of deep crustal structure of the Rehai geothermal field near Tengchong, southern China. Geophysical Journal International 147, 677–687.

Beattie, P., 1993. Uranium–thorium disequilibria and partitioning on melting of garnet peridotite. Nature 363, 63–65.

Ben Othman, D., White, W.M., Patchett, J., 1989. The geochemistry of marine sediments, island arc magma genesis, and crust–mantle recycling. Earth and Planetary Science Letters 94, 1–21.

Bourdon, B., Sims, K.W.W., Lundstrom, 2003. U-series constraints on intraplate basaltic magmatism. In: Bourdon, B., Henderson, G.M., Turner, S.P. (Eds.), Uranium-Series Geochemistry, pp. 215–254.

Chen, F., Satir, M., Ji, J., Zhong, D., 2002. Nd–Sr–Pb isotopes of Tengchong Cenozoic volcanic rocks from western Yunnan, China: evidence for an enriched-mantle source. Journal of Asian Earth Sciences 21, 39–45.

Chen, J.L., Xu, J.F., Wang, B.D., Kang, Z.Q., 2012. Cenozoic Mg-rich potassic rocks in the Tibetan Plateau: geochemical variations, heterogeneity of subcontinental lithospheric mantle and tectonic implications. Journal of Asian Earth Sciences 53, 115–130.

Cheng, H., Edwards, R.L., Hoff, J., Gallup, C.D., Richards, D.A., Asmerom, Y., 2000. The half-lives of uranium-234 and thorium-230. Chemical Geology 169, 17–33.

Chung, S., Chun, M., Zhang, Y., Xie, Y., Lo, C., Lee, T., Lan, C., Li, X., Zhang, Q., Wang, Y., 2005. Tibetan tectonic evolution inferred from spatial and temporal variations in post-collisional magmatism. Earth-Science Reviews 68, 24.

Cooper, K.M., Reid, M.R., Dunbar, N.W., McIntosh, W.C., 2002. Origin of mafic magmas beneath northwestern Tibet: constraints from ^{230}Th–^{238}U disequilibria. Geochemistry, Geophysics, Geosystems. http://dx.doi.org/10.1029/2002GC000332.

Ding, L., Kapp, P., Zhong, D., Deng, W., 2003. Cenozoic volcanism in Tibet: evidence for a transition from oceanic to continental subduction. Journal of Petrology 44, 33.

Dosseto, A., Bourdon, B., Joron, J., Dupre, B., 2003. U–Th–Pa–Ra study of the Kamchatka arc: new constraints on the genesis of arc lavas. Geochimica et Cosmochimica Acta 67, 21.

Elliott, T., 1997. Fractionation of U and Th during mantle melting: a reprise. Chemical Geology 139, 19.

Flower, M.F., Tamaki, K., Hoang, N., 1998. Mantle extrusion: a model for dispersed volcanism and DUPAL-like asthenosphere in East Asia and the West Pacific. In: Flower, M.F.J., Chung, S.L., Lo, C.H., Lee, T.Y. (Eds.), Mantle Dynamics and Plate Interaction in East Asia. Am. Geophys. Union, Washington, D. C., pp. 67–88.

Galer, S.J.G., O'Nions, R.K., 1985. Residence time of thorium, uranium and lead in the mantle with implications for mantle convection. Nature 316, 778–782.

Gao, Y.G., Hou, Z.Q., Kamber, B.S., Wei, R.H., Meng, X.J., Zhao, R.S., 2007. Lamproitic rocks from a continental collision zone: evidence for recycling of subducted Tethyan oceanic sediments in the mantle beneath southern Tibet. Journal of Petrology 48, 729–752.

Gao, Y.F., Wei, R.H., Ma, P.X., Hou, Z.Q., Yang, Z.S., 2009. Post-collisional ultrapotassic volcanism in the Tangra Yumco–Xuruco graben, south Tibet: constraints from geochemistry and Sr–Nd–Pb isotope. Lithos 110, 129–139.

George, R., Turner, S., Hawkesworth, C., Morris, J., Nye, C., Ryan, J., Zheng, S.-H., 2003. Melting processes and fluid and sediment transport rates along the Alaska–Aleutian arc from an integrated U–Th–Ra–Be isotope study. Journal of Geophysical Research 108, 25.

Govindaraju, K., 1994. 1994 compilation of working values and sample descriptions for 383 geostandards. Geostandards Newsletter 18, 15–53.

Guo, Z.F., Wilson, M., Liu, J.Q., Mao, Q., 2006. Post-collisional, potassic and ultrapotassic magmatism of the northern Tibetan Plateau: constraints on characteristics of the mantle source, geodynamic setting and uplift mechanisms. Journal of Petrology 47, 1177–1220.

Huang, P.G., Jiang, C.S., 2000. Study on Tengchong volcanic activity. Yunnan Science and Technology Press, Kunming (418 pp.).

Huang, J.L., Zhao, D.P., 2006. High-resolution mantle tomography of China and surrounding regions. Journal of Geophysical Research 111, B09305.

Jaffey, A.H., Flynn, K.F., Glendenin, L.E., Bentley, W.C., Essling, A.M., 1971. Precision measurement of half-lives and specific activities of U-235 and U-238. Physical Review C 4, 1889–1906.

Jiang, C., 1998. Stages of eruptions of the Tengchong volcanoes. Journal Seismological Research 21, 309–319.

Johnson, D.M., Hooper, P.R., Conrey, R.M., 1999. XRF Analysis of Rocks and Minerals for Major and Trace Elements on a Single Low Dilution Li-Tetraborate Fused Bead. JCPDS-International Centre for Diffraction Data 843–867.

Landwehr, D., Blundy, J., Chamorro-Perez, E.M., Hill, E., Wood, B., 2001. U-series disequilibrium generated by partial melting of spinel lherzolite. Earth and Planetary Science Letters 188, 329–348.

LaTourrette, T.Z., Kennedy, A.K., Wasserburg, G.J., 1993. Thorium–uranium fractionation by garnet: evidence for a deep source and rapid rise of oceanic basalts. Science 261, 739–742.

Lei, J.S., Zhao, D.P., Su, Y.J., 2009. Insight into the origin of the Tengchong intraplate volcano and seismotectonics in southwest China from local and teleseismic data. Journal of Geophysical Research 114, B05302 (05310.01029/02008JB005881).

Lei, J.S., Xie, F.R., Fan, Q.C., Santosh, M., 2013. Seismic imaging of the deep structure under the Chinese volcanoes: an overview. Physics of the Earth and Planetary Interiors 224, 104–123.

Li, D.M., Li, Q., Chen, W.J., 2000. Volcanic activity of Tengchong since the Pliocene. Acta Petrologica Sinica 16, 362–370.

Li, C., van der Hilst, R.D., Meltzer, A.S., Engdahl, E.R., 2008. Subduction of the Indian lithosphere beneath the Tibetan Plateau and Burma. Earth and Planetary Science Letters 274, 157–168.

Liu, R.X., Chen, W.J., Sun, J.Z., Li, D.M., 1992. The K-Ar age and tectonic environment of Cenozoic volcanic rocks in China. In: Liu, R.X. (Ed.), The Age and Geochemistry of Cenozoic Volcanic Rocks in China. Seismology Publishing House, pp. 1–43.

Lundstrom, C.C., 2003. Uranium-series disequilibria in Mid-Ocean Ridge Basalts: observations and models of basalt genesis. In: Bourdon, B., Henderson, G.M., Lundstrom, Turner, S.P. (Eds.), Uranium-Series Geochemistry, pp. 175–214.

Lundstrom, C.C., Shaw, H.F., Ryerson, F.J., Phinney, D.L., Gill, J.B., Williams, Q., 1994. Compositional controls on the partitioning of U, Th, Ba, Pb, Sr, and Zr between clinopyroxene and haplobasaltic melts: implications for uranium series disequilibria in basalts. Earth and Planetary Science Letters 128, 407–423.

McDonough, W.F., Sun, S.S., 1995. The composition of the Earth. Chemical Geology 120, 223–253.

McKenzie, D., 1985. ^{230}Th–^{238}U disequilibrium and the melting processes beneath ridge axes. Earth and Planetary Science Letters 72, 149–157.

Mo, X.X., Hou, Z.Q., Niu, Y.L., Dong, G.C., Qu, X.M., Zhao, Z.D., Yang, Z.M., 2007. Mantle contributions to crustal thickening during continental collision: evidence from Cenozoic igneous rocks in southern Tibet. Lithos 96, 225–242.

Mu, Z.G., Curtis, G.H., Liao, Z.J., Tong, W., 1987. K–Ar age and strontium isotopic composition of the Tengchong volcanic rocks, West Yunnan Province, China. Geothermics 16, 283–297.

Mukasa, S.B., Fischer, G.M., Barr, S.M., 1996. The character of the subcontinental mantle in southeast Asia: evidence from isotopic and elemental compositions of extension-related Cenozoic basalts in Thailand. In: Basu, A.R., Hart, S.R. (Eds.), Earth Processes: Reading the Isotopic Code. American Geophys. Union, Washington, pp. 233–252.

Peate, D.W., Hawkesworth, C.J., 2005. U series disequilibria: insights into mantle melting and the timescales of magma differentiation. Reviews of Geophysics 43, RG1003.

Pickett, D.A., Murrell, M.T., 1997. Observations of ^{231}Pa/^{235}U disequilibrium in volcanic rocks. Earth and Planetary Science Letters 148, 13.

Plank, T., Langmuir, C.H., 1988. An evaluation of the global variations in the major element chemistry of arc basalts. Earth and Planetary Science Letters 90, 22.

Plank, T., Langmuir, C.H., 1998. The chemical composition of subducting sediment and its consequences for the crust and mantle. Chemical Geology 145, 325–394.

Prelevic, D., Jacob, D.E., Foley, S.F., 2013. Recycling plus: a new recipe for the formation of Alpine–Himalayan orogenic mantle lithosphere. Earth and Planetary Science Letters 362, 187–197.

Rapp, R.P., Irifune, T., Shimizu, N., NIshiyama, N., Norman, M.D., Inoue, T., 2008. Subduction recycling of continental sediments and the origin of geochemically enriched reservoirs in the deep mantle. Earth and Planetary Science Letters 271, 14–23.

Rudnick, R.L., Gao, S., 2003. Composition of the continental crust. Treatise on Geochemistry 1–64.

Salters, V.J.M., Longhi, J., 1999. Trace element partitioning during the initial stages of melting beneath mid-ocean ridges. Earth and Planetary Science Letters 166, 15–30.

Sekine, T., Wyllie, P.J., 1983. Experimental simulation of mantle hybridization in subduction zones. Journal of Geology 91, 511–528.

Shen, C.-C., Edwards, R.L., Cheng, H., Dorale, J.A., Thomas, R.B., Moran, S.B., Weinstein, S.E., Edmonds, H.N., 2002. Uranium and thorium isotopic and concentration measurements by magnetic sector inductively coupled plasma mass spectrometry. Chemical Geology 185, 165–178.

Shen, C.-C., Cheng, H., Edwards, R.L., Moran, S.B., Edmonds, H.N., Hoff, J.A., Thomas, R.B., 2003. Measurement of attogram quantities of ^{231}Pa in dissolved and particulate fractions of seawater by isotope dilution thermal ionization mass spectrometry. Analytical Chemistry 75, 1075–1079.

Shen, C.-C., Wu, C.C., Cheng, H., Edwards, R.L., Hsieh, Y.T., Gallet, S., Chang, C.C., Li, T.Y., Lam, D.D., Kano, A., Hori, M., 2012. High-precision and high resolution carbonate ^{230}Th dating by MC-ICP-MS with SEM protocols. Geochimica et Cosmochiica Acta 99, 71–86.

Sigmarsson, O., Martin, H., Knowles, J., 1998. Melting of a subducting oceanic crust from U–Th disequilibria in austral Andean lavas. Nature 394, 566–569.

Sims, K.W.W., DePaolo, D.J., Murrell, M.T., Baldredge, W.S., Goldstein, S., Clague, D., Jull, M., 1999. Porosity of the melting zone and variations in the solid mantle upwelling rate beneath Hawaii: inferences from ^{238}U–^{230}Th–^{226}Ra and ^{235}U–^{231}Pa disequilibria. Geochimica et Cosmochimica Acta 63, 4119–4138.
Spiegelman, M., Elliott, T., 1993. Consequences of melt transport for uranium series disequilibrium in young lavas. Earth and Planetary Science Letters 118, 1–20.
Todt, W., Cliff, R.A., Hanser, A., Hofmann, A.W., 1996. Evaluation of a ^{202}Pb–^{205}Pb double spike for high-precision lead isotope analysis. In: Basu, A.R., Hart, S.R. (Eds.), Earth Processes: Reading the Isotopic Code. Geophysical Monograph Am. Geophys. Union, pp. 429–437.
Tu, K., Flower, M.F.J., Carlson, R.W., Zhang, M., Xie, G., 1991. Sr, Nd, and Pb isotopic compositions of Hainan basalts (south China): implications for a subcontinental lithosphere Dupal source. Geology 19, 567–569.
Tucker, R.T., Zou, H.B., Fan, Q.C., Schmitt, A.K., 2013. Ion microprobe dating of zircons from active Dayingshan volcano, Tengchong, SE Tibetan Plateau: time scales and nature of magma chamber storage. Lithos 172–173, 214–221.
Turner, S., Foden, J., 2001. U, Th and Ra disequilibria, Sr, Nd and Pb isotope and trace element variations in Sunda arc lavas: predominance of a subducted sediment component. Contributions to Mineralogy and Petrology 142, 43–57.
Turner, S.P., Arnaud, N., Liu, J., Rodgers, N., Hawkesworth, C., Harris, N., Kelley, S., Van Calsteren, P., Deng, W., 1996. Post-collision, shoshonitic volcanism on the Tibetan Plateau: implications for convective thinning of the lithosphere and the source of ocean island basalts. Journal of Petrology 37, 45–71.
Turner, S.P., Bourdon, B., Gill, J.B., 2003. Insights into magma genesis at convergent margins from U-series isotopes. In: Bourdon, B., Henderson, G.M., Lundstrom, C.C., Turner, S.P. (Eds.), Uranium-Series Geochemistry, pp. 255–310.
Wang, C.Y., Gang, H.F., 2004. Crustal structure in Tengchong volcano-geothermal area, western Yunnan, China. Tectonophysics 380, 69–87.
Wang, J.H., Yin, A., Harrison, T.M., Grove, M., Zhang, Y.Q., Xie, G.H., 2001. A tectonic model for Cenozoic igneous activities in the eastern Indo–Asian collision zone. Earth and Planetary Science Letters 188, 123–133.
Wang, F., Peng, Z.C., Zhu, R.X., He, H.Y., Yang, L.K., 2006. Petrogenesis and magma residence time of lavas from Tengchong volcanic field (China): evidence from U series disequilibria and $^{40}Ar/^{39}Ar$ dating. Geochemistry, Geophysics, Geosystems 7, Q01002 (01010.01029).
Williams, R.W., Collerson, K.D., Gill, J.B., Deniel, C., 1992. High Th/U ratios in subcontinental lithospheric mantle: mass spectrometric measurement of Th isotopes in Gaussberg lamproites. Earth and Planetary Science Letters 111, 257–268.
Williams, H.M., Turner, S.P., Peace, J.A., Kelley, S.P., Harris, N.B.W., 2004. Nature of the source regions for post-collisional, potassic magmatism in southern and northern Tibet from geochemical variations and inverse trace element modelling. Journal of Petrology 45, 555–607.
Wood, B.J., Blundy, J.D., Robinson, J.A.C., 1999. The role of clinopyroxene in generating U-series disequilibrium during mantle melting. Geochimica et Cosmochimica Acta 63, 1613–1620.
Yin, G.M., Li, S.H., 2000. The thermoluminescence dating of the last eruption of Tengchong volcano. Earthquake Research 23, 12–17.
Zhao, Y.W., Fan, Q.C., 2010. Magma origin and evolution of Maanshan volcano. Dayingshan volcano and Heikongshan volcano in Tengchong area. Acta Petrologica Sinica 26, 1133–1140.
Zhao, D.P., Liu, L., 2010. Deep structure and origin of active volcanoes in China. Geoscience Frontiers 1, 31–44.
Zhao, Z., Mo, X., Dilek, Y., Niu, Y., DePaolo, D.J., Robinson, P., Zhu, D., Sun, C., Dong, G., Zhou, S., Luo, Z., Hou, Z., 2009. Geochemical and Sr–Nd–Pb–O isotopic compositions of the post-collisional ultrapotassic magmatism in SW Tibet: petrogenesis and implications for India intra-continental subduction beneath southern Tibet. Lithos 113, 23.
Zhou, M.F., Robinson, P.T., Wang, C.Y., Zhao, J.H., Yan, D.P., Gao, J.F., Malpas, J., 2012. Heterogeneous mantle source and magma differentiation of quaternary arc-like volcanic rocks from Tengchong, SE margin of the Tibetan Plateau. Contributions to Mineralogy and Petrology 163, 841–860.
Zhu, B.Q., Mao, C.X., Lugmair, G.W., Macdougall, J.D., 1983. Isotopic and geochemical evidence for the origin of Plio-Pleistocene volcanic-rocks near the Indo–Eurasian collisional margin at Tengchong, China. Earth and Planetary Science Letters 65, 263–275.
Zindler, A., Hart, S.R., 1986. Chemical geodynamics. Annual Review of Earth and Planetary Sciences 14, 493–571.
Zou, H.B., 2007. Quantitative Geochemistry. Imperial College Press, London.
Zou, H.B., Fan, Q.C., 2010. U–Th isotopes in Hainan basalts: implications for sub-asthenospheric origin of EM2 mantle endmember and the dynamics of melting beneath Hainan Island. Lithos 116, 145–152.
Zou, H.B., Zindler, A., 2000. Theoretical studies of ^{238}U–^{230}Th–^{226}Ra and ^{231}Pa–^{235}U disequilibria in young lavas produced during mantle melting. Geochimica et Cosmochimica Acta 64, 1809–1817.
Zou, H.B., Zindler, A., Xu, X.S., Qi, Q., 2000. Major and trace element, and Nd–Sr–Pb isotope studies of Cenozoic basalts in SE China: mantle sources, regional variations, and tectonic significance. Chemical Geology 171, 33–47.
Zou, H.B., Reid, M.R., Liu, Y.S., Yao, Y.P., Xu, X.S., Fan, Q.C., 2003. Constraints on the origin of historic potassic basalts from northeast China by U–Th disequilibrium data. Chemical Geology 200, 189–201.
Zou, H.B., Fan, Q.C., Yao, Y.P., 2008. U–Th systematics of dispersed young volcanoes in NE China: asthenosphere upwelling caused by piling up and upward thickening of stagnant Pacific slab. Chemical Geology 255, 134–142.
Zou, H.B., Fan, Q.C., Schmitt, A.K., Sui, J.L., 2010. U–Th dating of zircons from Holocene potassic andesites (Maanshan volcano, Tengchong, SE Tibetan Plateau) by depth profiling: time scales and nature of magma storage. Lithos 118, 202–210.